Analysis of Small Spalling Mechanism on Hot Rolling Mill Roll Surface

Sonoda, Akio
Department of Mechanical Engineering Science, Kyushu University : Graduate Student

Hamada, Shigeru
Department of Mechanical Engineering, Kyushu University : Associate Professor

Noguchi, Hiroshi
Department of Mechanical Engineering, Kyushu University : Professor

Analysis of Small Spalling Mechanism on Hot Rolling Mill Roll Surface

by

Akio SONODA[*], Shigeru HAMADA[**]

and Hiroshi NOGUCHI[***]

Abstract

In order to analyze the small spalling mechanism on the surface of the hot rolling mill high speed steel roll, an actual hot rolling mill roll was investigated, and the thermal cycle and Mode II fatigue crack growth tests, which reflect the results of the investigation, were carried out. From the investigation of the actual hot rolling mill roll, it was proven that the small spalling was generated by heat crack initiation by thermal cycling and Mode II fatigue crack growth. The crack due to the thermal cycling was initiated in the oxide area. Estimation of the small spalling hot rolling mill roll life on the roll surface became possible based on the relationship between the crack growth rate da/dN and threshold Mode II stress intensity factor range ΔK_{IIth}, and it was clarified that the life of the Mode II fatigue crack growth was longer than that of the crack initiation life by thermal cycling.

Keywords: Hot rolling, Roll, Small spalling, Thermal crack, Mode II fatigue crack growth

1. Introduction

In a hot rolling mill, high speed steel, which has a high wear resistance, is used for the rolls, and the high speed steel rolls have an increase in roll life with improvement of the roll performance[1),2)]. However, in the hot rolling mill roll, there is a case which a crack initiates by thermal cycling on the roll surface, and this crack grows by mechanical loading[3),4)]. The roll surface becomes rough due to the crack growth and small spalling, which cause an increase in the roll regrinding thickness. In this study of high speed steel, which plays an important role in the hot rolling mill roll, the crack initiation by thermal cycling and the crack growth by mechanical loading were tested by dividing it into elements as factors of small spalling on the roll surface. The small spalling life of the actual hot rolling mill roll was then verified using the test results.

[*]   Graduate Student, Department of Mechanical Engineering Science
[**]   Associate Professor, Department of Mechanical Engineering
[***] Professor, Department of Mechanical Engineering

2.   Actual hot rolling mill roll investigation

2.1 Cross sectional observation of the small spalling place

Figure 1 shows the small spalling which exists on the hot rolling mill roll surface after 1.75×10^5 cycles. The roll diameter is 410mm. The finish processing of the roll surface was carried out by a grinding machine and surface roughness of the roll was Ra 1.0μm.

The crack depth is 1 - 2mm from the roll surface, and the size of the small spalling is about several mm - 10mm in the rotation's direction. Each small spalling connection to the rotation's direction was observed. The Hertzian pressure of P_0 = 1747MPa and contact half-width of c = 6.2mm were obtained from the rolling condition based on the elastic calculation. **Figure 2** shows the cross sectional observation of the small spalling site of the actual hot rolling mill roll. Some cracks perpendicular to the roll surface were observed, and one crack, which grew in the roll circumferential direction, was observed.
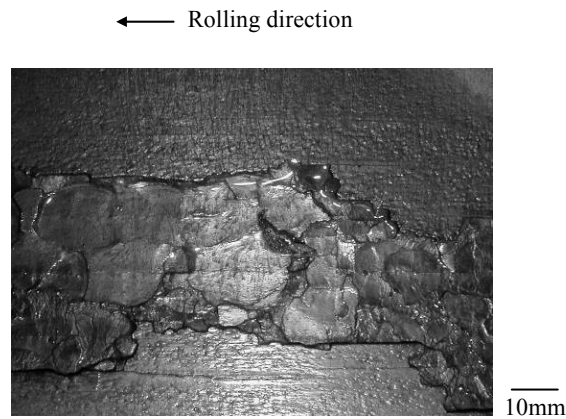
←—— Rolling direction

10mm

Fig.1 Small spalling of the hot rolling mill roll.
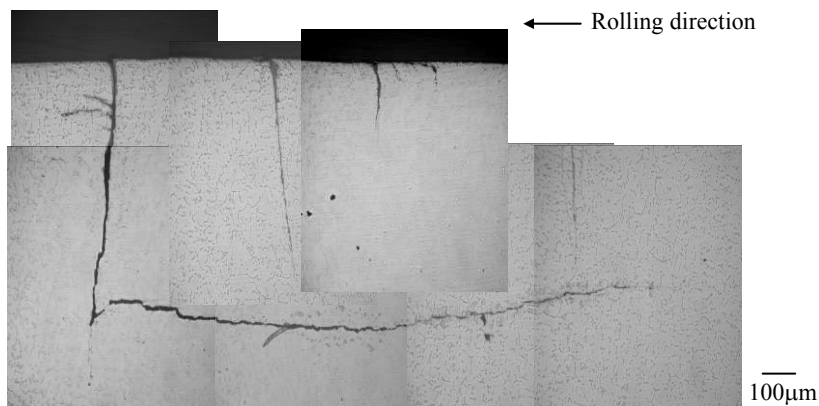
←—— Rolling direction

100μm

Fig.2   Cross section of the actual hot rolling mill roll.

2.2 Discussion of the small spalling

2.2.1 Cracks perpendicular to the roll surface

During rough rolling and finish front rolling, when the roll surface is rapidly cooled during rolling, cracks are initiated by tensile stress which act on the roll surface[3,4]. The tensile stress of the roll surface causes the perpendicular crack initiation on the roll surface. The observed crack shown in **Fig.2** has a shape similar to that reported in the literatures[3,4].

2.2.2 Circumferential crack on roll subsurface

Due to the rolling mechanical loading, the perpendicular crack seems to grow in the circumferential direction. The perpendicular crack is closed by the Hertzian pressure, because the stress field of the Hertzian contact region is compression[5]. When liquid from the outside does not enter to the crack surface as in a perpendicular crack, the crack shifts to a Mode II crack growth without causing Mode I crack growth[3]. The circumferential crack observed in **Fig.2** is thought to grow by the Mode II loading.

3.   Element tests of the small spalling

In this study, the perpendicular crack initiation seemed to be caused by thermal cycling, and the circumferential crack seemed to be caused by the Mode II fatigue crack growth. The crack initiation and propagation were separated, and the tests were carried out using the same hot rolling mill roll material. The specimen was cast in a $\phi 90 \times 400$ mm cylinder metal mold. For the thermal cycle test (described in section 3.1), the test sample was cut out in the direction of the longitudinally perpendicular plane as the test plane, and a specimen was longitudinally cut out for the Mode II fatigue crack growth test (described in section 3.2). They were formed in the specimen shape after hardening at 1000°C and tempering at 560°C were carried out. The mechanical properties of the specimen are shown in **Table 1**.

3.1 Thermal cycle test

Figure 3 shows the shapes and dimensions of the specimen and test method. The thermal cycling test carried out under the actual hot rolling roll condition: material and heating temperature and cooling method. The specimen of thermal cycling test is not a roll shape. In this study, we consider the effect of the thermal cycling for the material is able to be confirmed. The center of the specimen was heated for about 3 minutes by high frequency induction heating equipment until specimen surface temperature became 600°C. The equipment power was 3kW, and a high frequency induction coil ($\phi 20$mm) was used. The specimen was moved in 0.5 seconds and cooled by water after the heated region became 600°C under the control of the heating temperature measurement by a radiation thermometer. The thermal cycle test was carried out under the condition that a cycle was from the heating to the cooling. A color check was carried out on the specimens, and the crack initiation was confirmed by a visual observation.

Table 1 Mechanical properties of the specimen.

HV (kgf/mm^2)	σ_B (MPa)
540	836

HV : Vickers Hardness
σ_B : Ultimate Tensile Strength
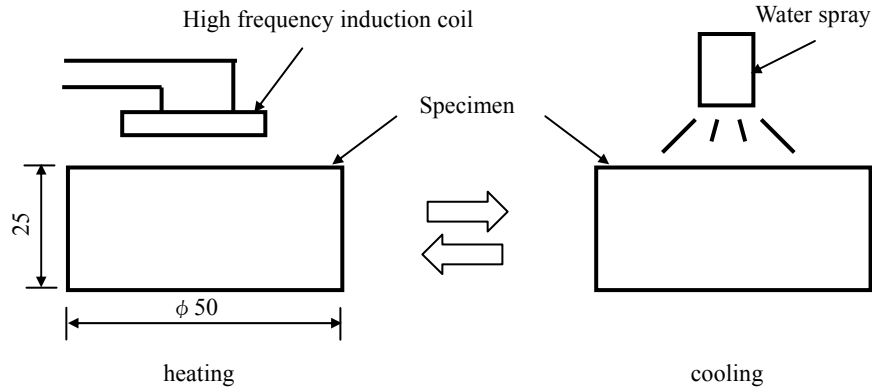
Fig.3 Thermal cycle test configuration and method.

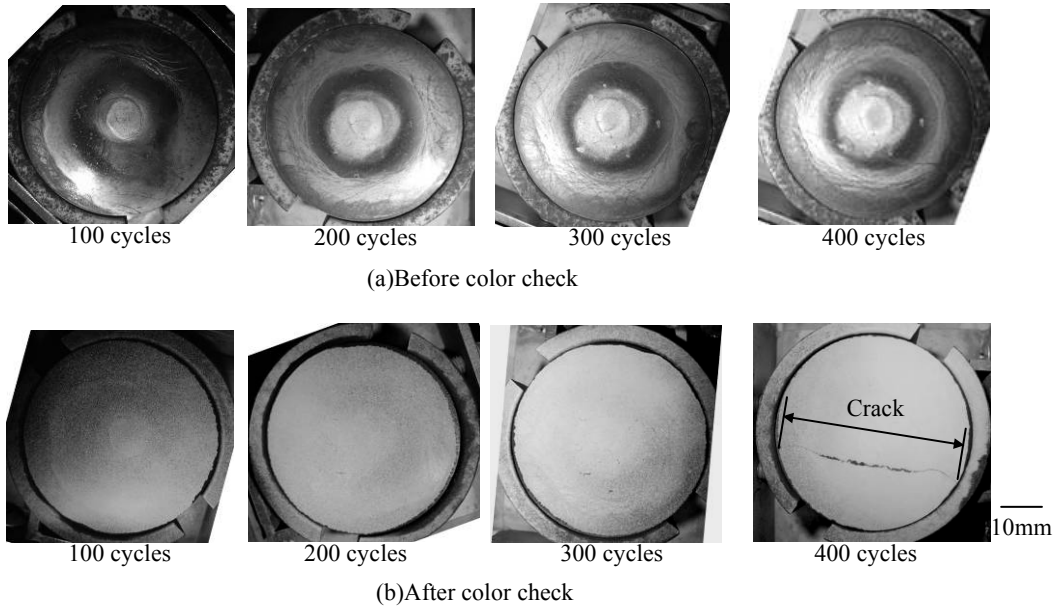(a)Before color check

(b)After color check

Fig.4 Specimen surface after thermal cycle test.

Figure 4 shows the surface state of the specimens after the thermal cycle test. The crack initiation was observed on the specimen surface after the thermal cycle test of 400 cycles.

3.2 Mode II fatigue crack growth test

Figure 5 shows the shapes and dimensions of the specimen. Murakami et al. developed the test method[6]. The specimen shape was devised in order to measure the Mode II fatigue crack growth using a general tension compression fatigue testing machine. The details of the test method have been described in the literature[6]. Two specimens are used in one test under the condition of the reversed tension - compression (stress ratio R = -1, load range ΔP = 12000N). The crack length was measured by the AC electrical potential method[7)-9)].
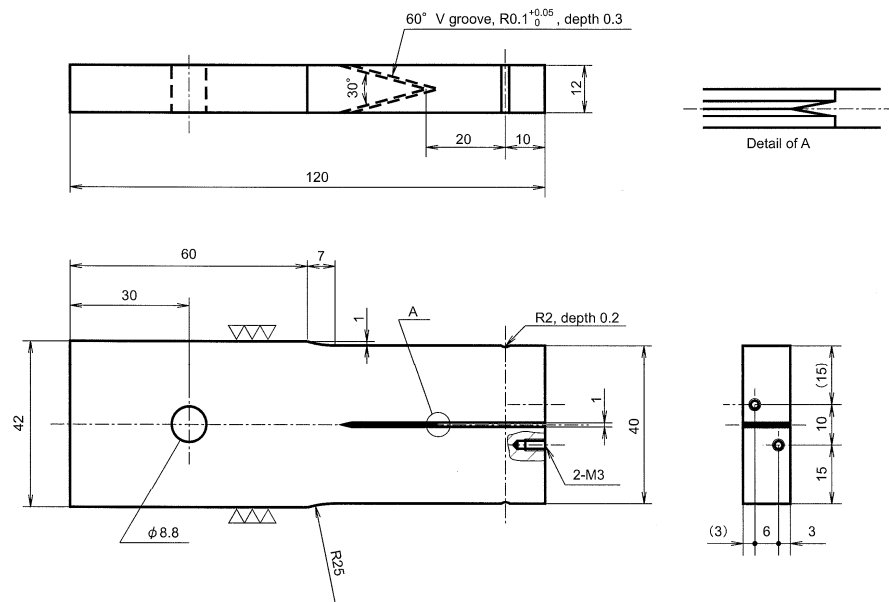
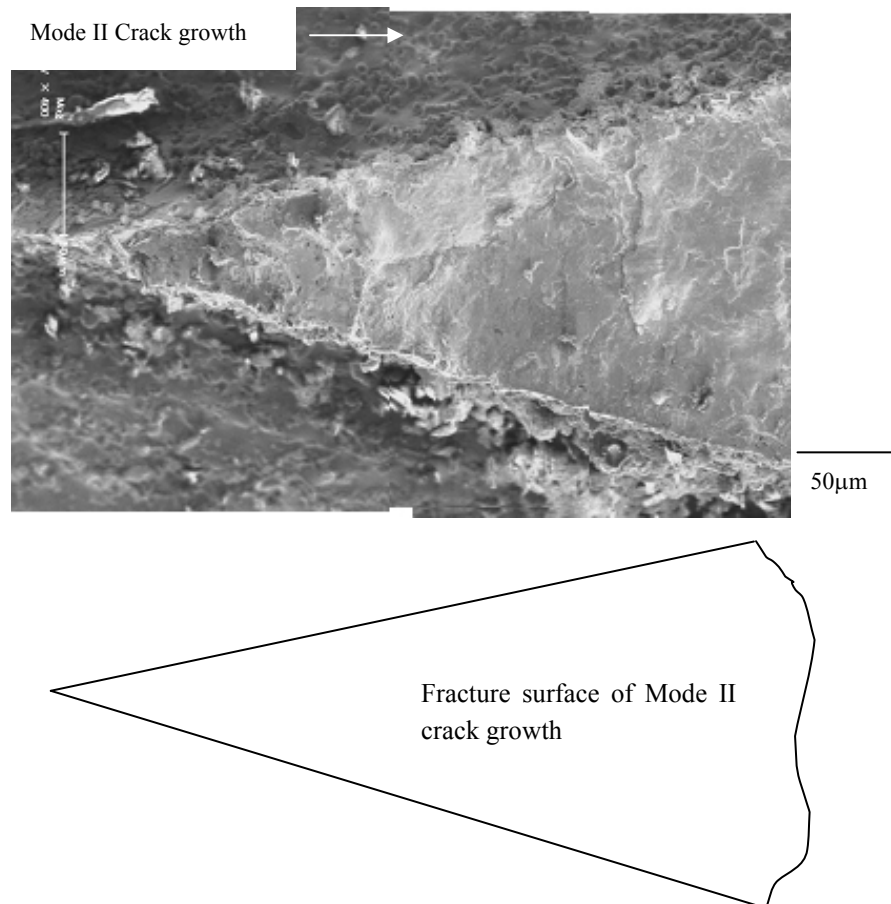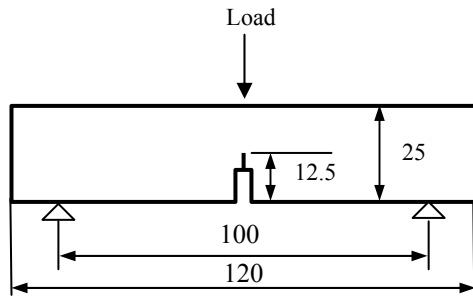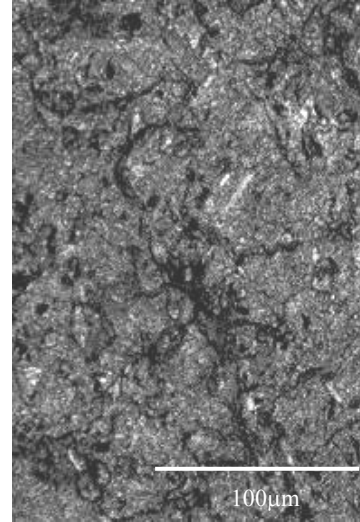**Fig.5** Shapes and dimensions of Mode II fatigue crack growth specimen[6].

Fig.6 Fracture surface of Mode II fatigue crack growth.

Load

25

12.5

100

120

specimen thicknes：12.5

(a) Shapes and dimensions of Mode I fatigue crack growth specimen.

Mode I Crack growth ⟶

100μm

(b) Fracture surface of Mode I fatigue crack growth.
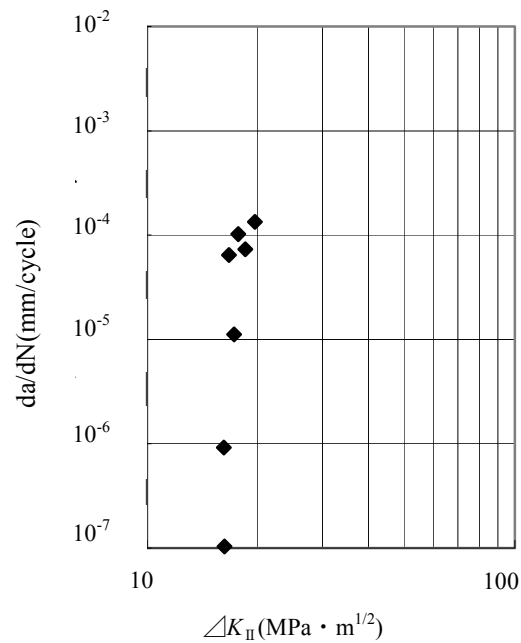
Fig.7   Mode I fatigue crack growth test.

da/dN(mm/cycle)

10^{-2}

10^{-3}

10^{-4}

10^{-5}

10^{-6}

10^{-7}

10

100

$\triangle K_{\mathrm{II}}(\mathrm{MPa} \cdot \mathrm{m}^{1/2})$

Fig.8   Relationship between crack growth rate, da/dN and Mode II stress intensity factor range, ΔK_{II}.

Figure 6 shows the fracture surface of the Mode II fatigue crack growth. The fracture surface is obviously different from the fracture surface of the Mode I fatigue crack growth ($R = 0.3$, $\Delta P = 2500N$) shown in **Fig.7**. Hamada's analysis results[10] were used for the calculation of the Mode II stress intensity factor range ΔK_{II}. **Figure 8** shows the relationship between the Mode II crack growth rate da/dN and ΔK_{II}. The Mode II threshold stress intensity factor range of $\Delta K_{IIth} = 16.0$ MPa$\sqrt{m}$ was obtained.

4. Discussion

4.1 Verification of the crack initiation by thermal cycling

Figure 9 is a photograph around the crack in the specimen surface observed after 400 cycles during the thermal cycle test. The crack growth was observed along the pattern of the black network. **Figure 10** shows the result of the analysis of this black network by EDX (Energy Dispersive X-ray spectroscopy). **Figure 10** shows the result of the oxygen analysis, and it was confirmed that oxygen existed in the black network. The oxide was generated, because the black network was a boundary of the dendrite, and the boundary is easy to be corroded in comparison to the matrix. **Figure 11** shows the result of EDX analysis and the position is different from the **Fig.10**. There are element peaks such as Fe, O and V. The compound oxide seems to have been formed. The Vickers hardness of the black network and the matrix was measured. The sizes of the indentations were about 25 μm under the load condition of 0.2kgf. As a result of the measurement, The Vickers hardness of the black network and the matrix were 680 and 460, respectively. The hardness of the black network is higher than that of the matrix. Based on this result, the black network becomes brittle due to the formation of the oxide.

In the actual hot rolling, the temperature of the rolled steel is 900-1000°C, and the oxide has been formed on the surface. Even if the oxide formed on the roll surface adhered to the rolled steel, the adherent oxide is finally removed with the oxide formed on the rolled steel. The oxide formed on the roll surface does not influence the product quality.

Figure 12 shows the color checked specimen after 300 thermal cycles. Some small cracks were observed on the specimen surface. Their length was about 2mm. **Figure 13** shows one of these cracks. A small crack was observed along the black network, and the crack length was about 2.5mm. In order to confirm the effect of the difference in the mechanical property of the same material, the same thermal cycle test was carried out to an HV370 specimen tempered at 600°C. **Figure 14** shows the thermal cycle test result for the HV370 specimen. Though in the HV370 specimen, no large crack as shown in **Fig.4**(b) (at 400 cycles) was observed after 700 cycles, the small crack as shown in **Fig.12** was mainly observed.

Verification on the condition of the crack initiation of the small crack origin was then carried out. Based on the calculation by the authors[11], in the specimen of the same material, the largest thermal tension stress, which acts on the surface of the specimen, was about 500MPa after 0.2 seconds from the starts of cooling from 600°C. The Mode I stress intensity factor K_I was calculated using the following equation by considering the effect of the inclusion, when the small crack (the overall length $2a = 2.5mm$) as in **Fig.13** was initiated by the effect of the oxide during the thermal cycle. The effect by the sliding in actual hot rolling was not considered, because the contact area between the rolled steel and the hot rolling mill roll was far from a cooled area of the roll surface.

$$K_I = \sigma\sqrt{\pi(a + \sqrt{area}_{max})} \tag{1}$$

The crack depth a was considered to be half of the crack's overall length. The largest inclusion length $\sqrt{area}_{max}$ was estimated by the statistics of extreme[12]. The critical volume V was considered

using the following equation by considering the effect of the high frequency heating depth (the depth is 1.8mm in this study).

$$V = S \times h_h \tag{2}$$

(*S*: Heating area, h_h =1.8mm: effect of the high frequency heating depth)

Figure 15 shows the result of the statistics of extreme. From **Fig.15**, the largest inclusion length estimated in the critical volume were 803μm. $K_I = 40.1\,\text{MPa}\sqrt{\text{m}}$ was obtained by substituting $\sigma = 500\text{MPa}$ and $a = 1.25\text{mm}$ and $\sqrt{area}_{max} = 803\text{μm}$ into Eq.(1). **Table 2** shows the fracture toughness values K_I of the HV540 specimen and HV370 specimen obtained from the fracture toughness test in **Fig.7** and **Fig.16**. For the HV540 specimen, $K_I = 38.1\,\text{MPa}\sqrt{\text{m}}$ is bigger than $K_{IC} = 33.0\,\text{MPa}\sqrt{\text{m}}$, and in the HV370 specimen, K_I is almost equal to $K_{IC} = 40.2\,\text{MPa}\sqrt{\text{m}}$. K_I becomes a maximum ($K_I = 40.1\,\text{MPa}\sqrt{\text{m}}$), when the inclusion close to the small crack exists as shown in **Fig.17**. In the thermal cycling test, it was estimated the small crack and the inclusion as shown in **Fig.17** did not exist. The small crack did not become a large crack because K_I is smaller than $K_{IC} = 40.2\,\text{MPa}\sqrt{\text{m}}$. In the HV370 specimen, the large crack was not observed after thermal cycle test in 700 cycles, but it is considered that the large crack is caused by the small crack and the inclusion as **Fig.17**, when the thermal cycle test is continuously carried out.
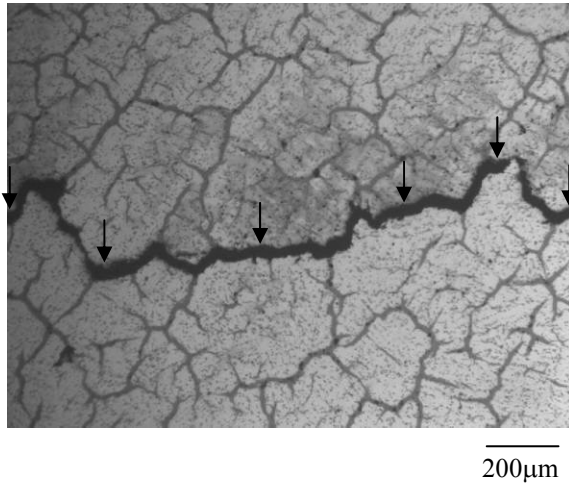

200μm

20μm

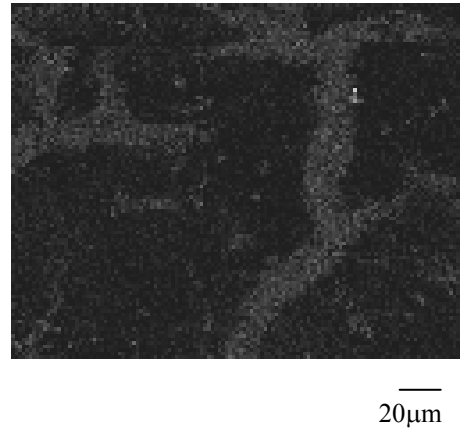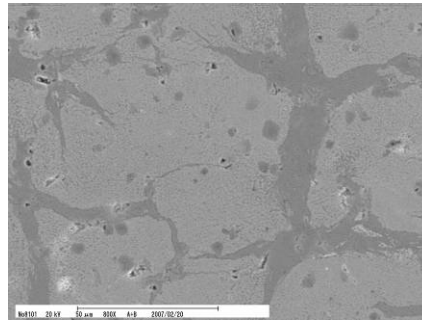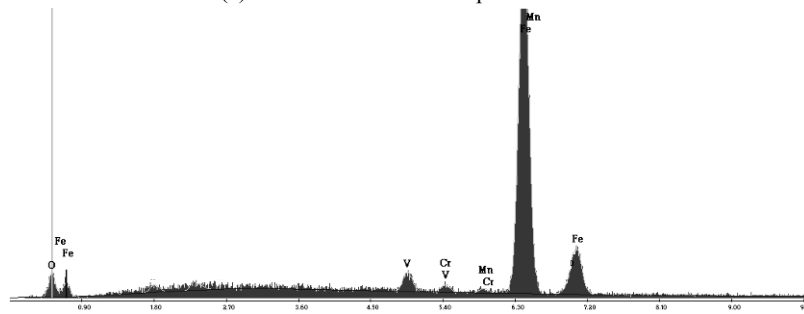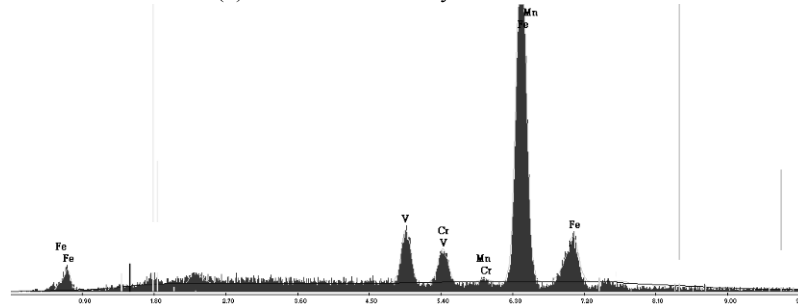**Fig.9** Crack on the thermal cycle specimen surface.   **Fig.10** Result of oxygen analysis on the specimen surface by EDX.
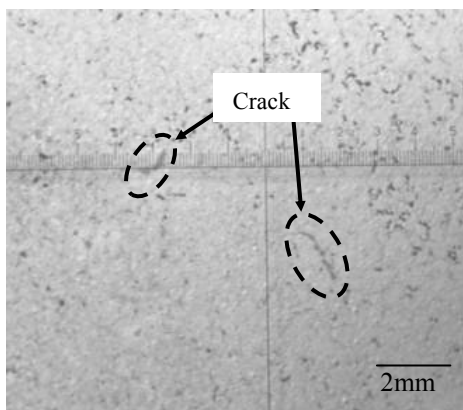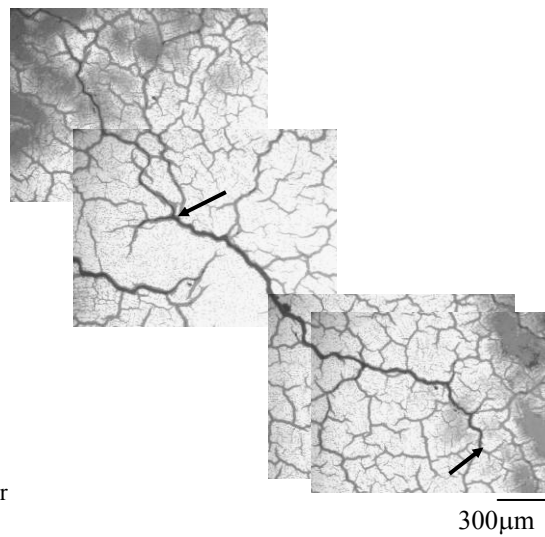
(a) Black network on the specimen surface.
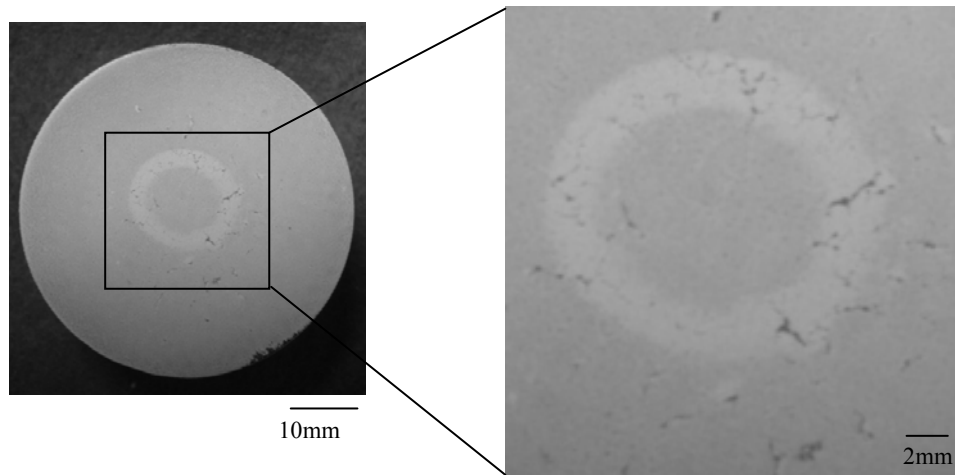

(b) Result of EDX analysis at black network.

(c) Result of EDX analysis at matrix.

Fig.11 Result of EDX analysis.

Crack

2mm

Fig.12 Small crack on the specimen surface after
300 thermal cycles.

300μm

Fig.13 Enlargement of the small crack.

(a) Specimen surface after thermal cycle test.   (b) Center of the specimen.

Fig.14 Small crack of HV370 specimen surface after 700 thermal cycles (black line in
(b) are small crack).

Table 2 Fracture toughness value.

HV (kgf/mm^2)	K_{IC} (MPa$\sqrt{m}$)
540	33.0
370	40.2

HV : Vickers Hardness
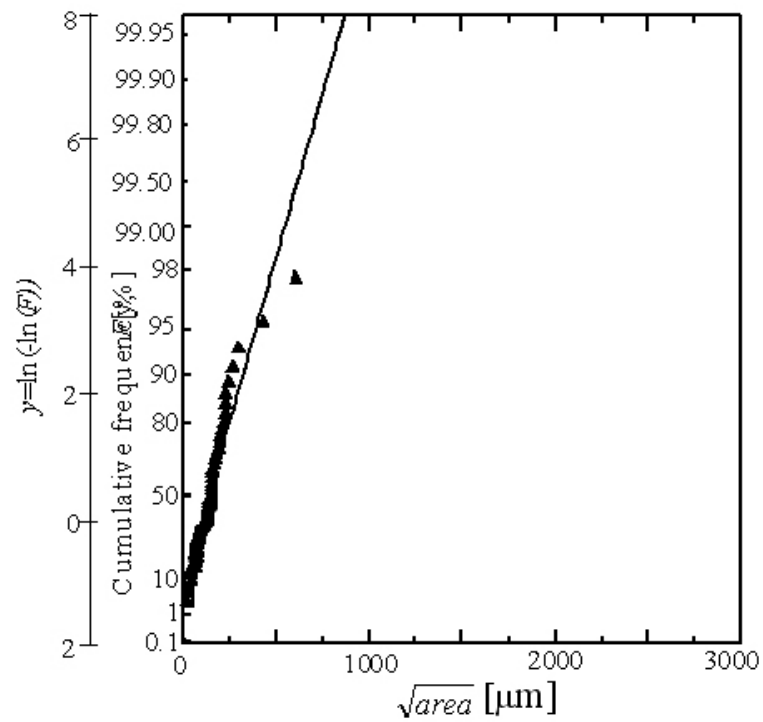K_{IC}: Fracture Toughness

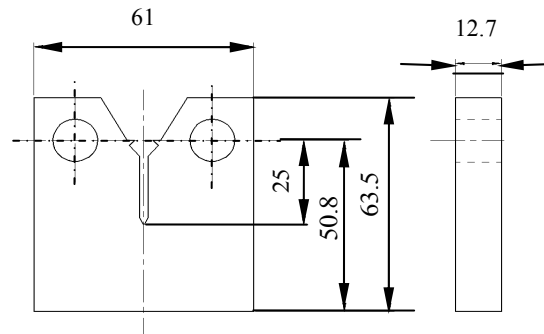**Fig.15** Result of statistics of extreme.

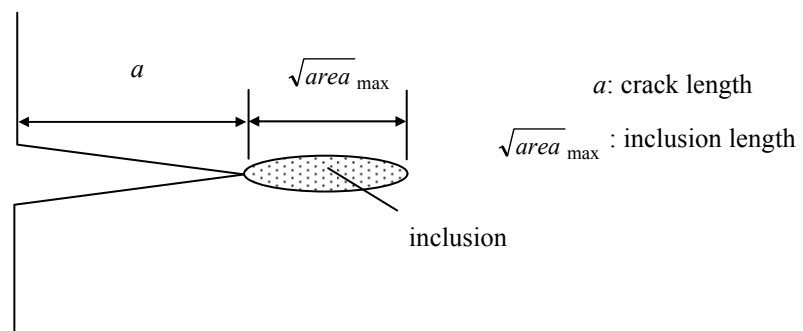**Fig.16** Shapes and dimensions of the fracture toughness test specimen.

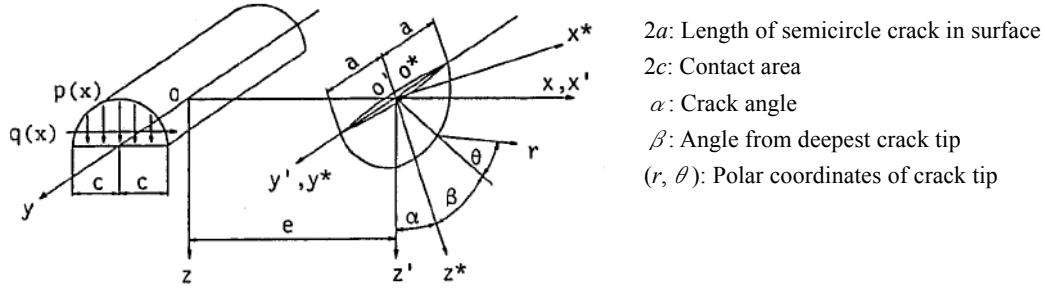**Fig.17** Inclusion close to small crack.

Fig.18 Analytical model and polar coordinates of crack tip[5].

$2a$: Length of semicircle crack in surface
$2c$: Contact area
α: Crack angle
β: Angle from deepest crack tip
(r, θ): Polar coordinates of crack tip

4.2 Verification of Mode II fatigue crack growth

4.2.1 Calculation of ΔK_{II} in the hot rolling mill roll

Using the analytical model of Murakami *et al.*[5] shown in **Fig.18**, the stress intensity factor in the vertical crack ($\alpha = 0°$) in the hot rolling mill roll was calculated. The calculation of Murakami *et al.* disregarded following effects: the pressure index of viscosity and compressibility and viscosity of penetrated liquid to the crack surface, and sliding, and the material change by the increase in the contact. In this paper, it is considered these effects can be disregarded to calculate the stress intensity factor at circumferential crack tip. In addition, the validity of the calculation of Murakami *et al.* has been confirmed by the calculation of Yamamoto *et al* [4]. The Hertzian pressure P_0 = 1747MPa and contact half-width c = 6.2mm in the hot rolling mill roll were considered. Calculating plastic deformation is difficult in the rolled steel. But we consider stress caused by elastic deformation is similar to the stress caused by elastic and plastic deformation. Then, in this study, the Hertz pressure obtained by the elasticity calculation is used.

When the crack length was considered a = 0.8mm was observed in **Fig.2**, and the friction coefficient was found to be f = 0.1, the Mode II stress intensity factor range, $\Delta K_{II} = 17.5\,\mathrm{MPa}\sqrt{\mathrm{m}}$, was obtained. The friction coefficient f = 0.1 referred to the literature[13] measured the friction coefficient in the rolling actually. The $\Delta K_{II} = 17.5\,\mathrm{MPa}\sqrt{\mathrm{m}}$ value obtained by the calculation exceeded $\Delta K_{IIth} = 16.0\,\mathrm{MPa}\sqrt{\mathrm{m}}$ of the specimen in **Fig.8**, and it satisfied the circumferential Mode II fatigue crack growth conditions.

4.2.2 Estimation of the small spalling life

When the circumferential the Mode II fatigue crack grew under the condition at ΔK_{II} = $17.5\,\mathrm{MPa}\sqrt{\mathrm{m}}$, Mode II fatigue crack growth rate $da/dN \approx 5.00\mathrm{x}10^{-5}$ mm/cycle was obtained from **Fig.8**. The circumferential crack length is 1.8mm in **Fig.2**. The life for the circumferential crack growth in **Fig.2** was estimated to be about $3.60\mathrm{x}10^4$ cycles. The hot rolling mill roll in **Fig.2** passed through $1.75\mathrm{x}10^5$ cycles, and small spalling was observed even during the 10^4 cycles (no crack growth was observed). The small spalling life is about $2.00\mathrm{x}10^5$ cycles, if the small spalling size is considered to be about 10 mm in **Fig.1**, and it approaches the phenomenon observed in the actual hot rolling mill roll. The circumferential crack growth length of **Fig.1** and **Fig.2** is different. If the circumferential crack started to grow, when the hot rolling mill roll started to use, there is the difference between the small spalling life prediction from **Fig.1** and the small spalling life prediction from **Fig.2**. Because the crack growth starting to the circumferential direction is uncertain, the estimation in the detailed crack growth life by the confirmation of the conversion of the perpendicular crack to the circumferential crack is required.

The crack initiation life by thermal cycling is then dependent on the material and rolling condition[15),16)]. In a similar material of the actual hot rolling mill roll, it is considered that $T_{thermal} \ll T_{ModeII}$ ($T_{thermal}$: crack initiation life by thermal cycling, T_{ModeII}: circumferential Mode II fatigue crack growth life). **Figure 19** shows the FEM analysis result[11)] of the thermal stress in the specimen from 600°C cooling. The material of specimen and material of the actual hot rolling mill roll are the same. In 1-2mm from the surface, the thermal stress hardly acts on. It is considered the thermal stress does not influence crack growth and crack opening, because the depth of the crack tip by the thermal cycling is 1-2mm.

The reprocessing of the hot rolling mill roll is carried out because the rough surface of the roll by the small spalling causes the print to the product. The roughness by the cracks on the thermal cycling is small, and the roughness does not cause the print to the product. The rolling process is possible to continue, if the cracks by the thermal cycling are generated on the roll surface.
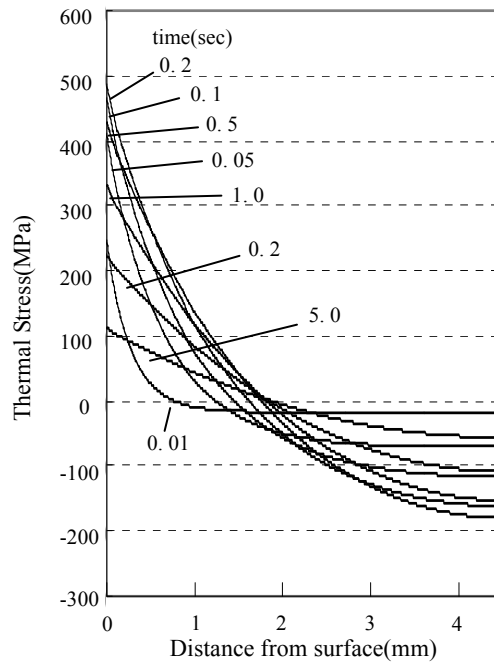

Fig.19 FEM analytical result of the thermal stress[11)].

5.　Conclusion

In this study, the actual high speed steel hot rolling mill roll was investigated. The high speed steel becomes important as the hot rolling mill roll. Considering the investigation of the actual hot rolling mill roll, the thermal cycle test and the Mode II fatigue crack growth test were carried out. The main results are as follows.

(1)　The oxide affected the crack initiation during the thermal cycling.

(2)　The Mode II fatigue crack growth rate for the high speed steel was obtained.

(3)　It was possible to estimate the small spalling life on the roll surface to some extent from the relationship da/dN and ΔK_{II}. This result is an index of the material development for high wear resistance materials like the high speed steel.

(4) Based on the results of the test results of the thermal cycle test and Mode II fatigue crack
     growth test, the small spalling life of the hot rolling mill roll was verified. The Mode II fatigue
     crack growth life was longer than the crack initiation life by thermal cycling.

References

1)   Rolling mill roll workshop ed., WHAT'S NEW IN ROLL TECHNOLOGIES OF THE
     WORLD, The Iron and Steel Institute of Japan (1995).
2)   M. Hashimoto, T. Kawakami, T. Oda, R. Kurahashi and K. Hokimoto, Development and
     Application of High-speed Tool Steel Roll in Hot Strip Rolling, NIPPON STEEL technical
     report, No.356 , pp.76-83 (1995).
3)   Y. Sano, D. Ching and E. Matsunaga, Analysis of Propagation of Surface Cracks of Work Roll
     for Hot Strip Mills, Transactions of JSME, Series C, Vol.58, No.552 , pp.248-253 (1992).
4)   H. Yamamoto, S. Uchida and M. Hashimoto, Numerical Analysis of Stress Intensity Factor of
     Crack in Subsurface Layer of Work Roll for Rolling, Tetsu-to-Hagane, Vol.83, No.7, pp.13-18
     (1997).
5)   Y. Murakami, M. Kaneta and H. Yatsuzuka, Analysis of Surface Cracking in Lubricated
     Rolling Contact), Transactions of JSME, Series C, Vol. 51, No.467, pp.1603-1611 (1985).
6)   Y. Murakami, S. Hamada, K. Sugino and K. Takao, New Measurement Method of Mode II
     Threshold Stress Intensity Factor Range $\Delta K_{\tau th}$ and Its Application, Journal of the Society of
     Materials Science, Japan, Vo.43, pp.1264-1270 (1994).
7)   T. Miyoshi and S. Nakano, A Study of the Determination of Surface Crack Shape by the
     Electric Potential Method, Transactions of JSME, Series A, Vol.52, No.476, pp.1097-1104
     (1986).
8)   K. Tanaka, Y. Akiniwa and S. Fujita, AC Electrical Potential Measurement of Fatigue Crack
     Growth in Notched Specimen, Journal of the Society of Materials Science, Japan, Vol.36,
     No.401, pp.177-183 (1987).
9)   Y. Nakai, H. Akagi, Y. Kitamura and K. Ohji, Measurement of Short Surface Crack Lengths
     by an AC Potential Method, Transactions of JSME, Series A, Vol.55, No.511, pp.543-549
     (1989).
10) S. Hamada, A Study of the Shear Type Fatigue Crack Growth, Dissertation, Kyushu Univ.,
     pp.67-76 (1997), [in Japanese].
11) A. Sonoda, S. Kashiwagi, S. Hamada and H. Noguchi, Quantitative Evaluation of Heat Crack
     Initiation Condition Under Thermal Shock, Journal of Solid Mechanics and Materials
     Engineering, Vo.2, No.1, pp.128-136 (2008).
12) Y. Murakami, Metal fatigue: effects of small defects and nonmetallic inclusions, Yokendo Ltd.,
     pp.15-23, pp.233-252 (1993).
13) T. Yoneyama and Y. Hatamura, Measurement of Actual Stress and Temperature on the Roll
     Surface in Hot Rolling (4th Report, Measurement of Actual Stress and Temperature on the
     Roll Surface in Hot Rolling), Transactions of JSME, Series C, Vol.56, No.527, pp.1935-1939
     (1990).
14) Y. Sano and K. Kimura, Statistical Analysis about Crack and Spalling on Work Roll for Hot
     Strip Mill Finishing Rear Stands, Tetsu-to-Hagane, Vol.73, No.9, pp.78-85 (1987).
15) Y. Sano and T. Hattori, Comments on "Formation and Falling Mechanism of Black Oxide
     Layers in High Speed Steel Rolls during Hot Strip Milling", Tetsu-to-Hagane, Vol.84, No.9,
     pp.77-79 (1998).